

Localization persisting under aperiodic drivingHongzheng Zhao^{1,2}, Florian Mintert,² Johannes Knolle,^{3,4,2} and Roderich Moessner¹¹Max-Planck-Institut für Physik komplexer Systeme, Nöthnitzer Straße 38, 01187 Dresden, Germany²Blackett Laboratory, Imperial College London, London SW7 2AZ, United Kingdom³Department of Physics TQM, Technische Universität München, James-Frank-Straße 1, D-85748 Garching, Germany⁴Munich Center for Quantum Science and Technology (MCQST), D-80799 Munich, Germany

(Received 26 November 2021; revised 5 February 2022; accepted 23 May 2022; published 6 June 2022)

Localization may survive in periodically driven (Floquet) quantum systems, but is generally unstable for aperiodic drives. In this Letter, we identify a hidden conservation law originating from a chiral symmetry in a disordered spin- $\frac{1}{2}$ XX chain. This protects indefinitely long-lived localization for general—even aperiodic—drives. Therefore, rather counterintuitively, adding further potential disorder which spoils the conservation law *delocalizes* the system, via a controllable parametrically long-lived prethermal regime. This provides an example of persistent single-particle “localization without eigenstates.”

DOI: [10.1103/PhysRevB.105.L220202](https://doi.org/10.1103/PhysRevB.105.L220202)

Introduction. Closed quantum many-body systems with time-dependent (“driven”) Hamiltonians tend to absorb energy until they reach a featureless “infinite temperature” state [1–3]. This heat death can be prevented if a sufficient number of integrals of motion is present. This may occur in integrable systems [4], or via the emergent structure underpinning many-body localization [5], which is stable against periodic driving for sufficiently strong disorder [6,7]. This even allows for novel nonequilibrium phenomena such as discrete-time crystalline order [8,9] and anomalous Floquet-Anderson insulators [10].

In recent years, the focus has shifted to aperiodic drives to control quantum systems [11–22]. This leads to new types of dynamical phenomena, e.g., nonadiabatic topological energy pumps [23–25] and prethermalization with algebraically scaling lifetimes [26,27]. However, the absence of time translation symmetry (TTS) is generally expected to generate stronger heating effects, in particular destabilizing localization [12,13]. Nonetheless, localization has been shown to remain robust for two-tone continuous drives [14], paving the way to stabilize nonequilibrium phases unobtainable with periodic drives, e.g., the quantum Hall effect in synthetic dimension [15–18] and discrete-time quasicrystals [12,13,19].

One natural question, then, is under what conditions can localization indefinitely survive generic aperiodic and even random driving profiles? Unlike multitone drives with few frequency components [12,14], generic drives contain low-frequency components which normally induce delocalization. Technically (and conceptually), the analysis of generic aperi-

odic drives is complicated as no way is known of analyzing the quantum dynamics in terms of a fixed set of eigenstates, $\{|\psi_i\rangle\}$, whose time evolution is described by a simple phase accumulation rate given by their respective (quasi)energies ϵ_i . Here, we show that a localized steady state can emerge in a noninteracting multiparticle system subjected to a drive with a well-defined coupling operator but general time dependence, and in this sense represents single-particle localization without eigenstates.

Our model hosts disorder not as an on-site potential but instead via randomness in the exchange interactions (or hopping amplitudes for fermions) [28,29,29,30]. The disordered exchange interaction has a single-particle chiral symmetry resulting in a spectrum symmetric around zero. Unlike the single-particle localization induced by potential disorder, where all eigenstates are localized, the chiral symmetric randomness does not fully localize all eigenstates, but instead yields a diverging localization length at zero energy [31–34]. Crucially, this chiral symmetry enables us to construct drives with a hidden conservation law, and we demonstrate that the localized steady state persists indefinitely for arbitrary aperiodic drives as long as the conservation law is preserved.

A static disorder-free exchange without the chiral symmetry, or potential disorder, destroys this feature. They do so via different routes, as the latter counterintuitively combines the *addition* of disorder with *delocalization* as the symmetry is broken. This “competition” gives rise, as a function of disorder strength, to a nonmonotonic heating rate. The resultant “prethermal” localized state can also be exceptionally long lived upon increasing the driving frequency.

In the following, we first introduce the model with the single-particle chiral symmetry, and show that the system reduces to a collection of two-level systems. Each pair corresponds to the localized chiral symmetric excitations at opposite energies $\pm\epsilon_i$. We then construct a drive which only introduces dynamics within each two-level system. Therefore, single-particle localization always persists despite the absence

Published by the American Physical Society under the terms of the [Creative Commons Attribution 4.0 International](https://creativecommons.org/licenses/by/4.0/) license. Further distribution of this work must maintain attribution to the author(s) and the published article's title, journal citation, and DOI. Open access publication funded by the Max Planck Society.

of well-defined eigenstates for generic aperiodic drives. For a multiparticle state, however, the single-particle chiral symmetry does not straightforwardly generalize. Instead, we show that it leads to an extensive number of local conserved quantities which can protect the multiparticle steady state from delocalization.

We then focus on the aperiodic Thue-Morse (TM) drive to numerically verify the existence of persistent localization via analyzing both the single-particle time evolution operator and the entanglement generation for multiparticle states. We finally show how different types of chiral symmetry-breaking perturbations lead to a long-lived prethermal regime with *non-monotonic* scalings of the prethermal lifetime.

The model and hidden conservation law. We focus on the spin- $\frac{1}{2}$ model described by the Hamiltonian

$$H(t) = H_0 + \delta h f(t) \hat{P}, \quad (1)$$

where the nearest-neighbor exchange interaction reads $H_0 = \frac{1}{4} \sum_i J_i (\sigma_i^x \sigma_{i+1}^x + \sigma_i^y \sigma_{i+1}^y)$ with disordered coupling strength $J_i \in [J_0, J_0 + J_{\max}]$. The staggered potential $\hat{P} = \sum_i (-1)^i \sigma_i^z / 2$ is modulated with the amplitude δh according to a time-dependent function $f(t)$ which will be specified later. Since $[H_0, \hat{P}] \neq 0$, the drive is not trivially equivalent to a quench. This model can be transformed into a noninteracting fermionic form [Eq. (2)] via the Jordan-Wigner transformation [35]

$$H(t) = \sum_i \frac{J_i}{2} (c_i^\dagger c_{i+1} + \text{H.c.}) + \delta h f(t) \sum_i (-1)^i n_i, \quad (2)$$

with the standard fermionic operators $c_i^{(\dagger)}$ and the number operator n_i . The model has a $U(1)$ symmetry, hence, the total particle number, or the total magnetization in spin language, is conserved. As the nearest-neighbor hopping is disordered, eigenstates of H_0 are localized (or quasilocated if the corresponding eigenenergies are close to zero [36,37]). As shown in the following, the Hamiltonian H_0 has a hidden conservation law even in the presence of \hat{P} which can protect the system from delocalizing regardless of the driving profile $f(t)$.

This conservation law originates from a single-particle chiral symmetry of the Hamiltonian H_0 . Considering a general real quadratic Hamiltonian $H_C = \sum_{ij} c_i^\dagger A_{ij} c_j$, its anticommutator with the staggered potential $\hat{P} = \sum_i (-1)^i n_i$ reads

$$\{H_C, \hat{P}\} = \sum_{ij} [(-1)^i + (-1)^j] A_{ij} c_i^\dagger c_j + \hat{D}, \quad (3)$$

with $\hat{D} = 2 \sum_{ijk} (-1)^k A_{ij} c_i^\dagger n_k c_j$. Crucially, the matrix elements of \hat{D} can be nonzero only for multiparticle states, but they vanish in the single-particle subspace. In addition, for the Hamiltonian H_0 considered in Eq. (1), the first contribution on the right-hand side of Eq. (3) vanishes because A_{ij} is nonzero only for $j = i + 1$; in this case, however, the corresponding prefactor $(-1)^i + (-1)^j$ vanishes. The anticommutator $\{H_0, \hat{P}\}$ thus vanishes in the single-particle subspace, which implies that the Hamiltonian H_0 is single-particle chiral symmetric: For a given single-particle eigenstate $|\epsilon_k\rangle$ of eigenenergy ϵ_k , $\hat{P} |\epsilon_k\rangle$ is also an eigenstate of opposite energy $-\epsilon_k$.

The Hamiltonian H_0 can thus be formally diagonalized as $H_0 = \sum_{0 < k \leq L/2} \epsilon_k \gamma_k^\dagger \gamma_k - \epsilon_k \tilde{\gamma}_k^\dagger \tilde{\gamma}_k$ with a new set of fermionic operators $\gamma_k, \tilde{\gamma}_k$ defined as

$$\gamma_k^\dagger = \sum_i V_{ki} c_i^\dagger, \quad \tilde{\gamma}_k^\dagger = \sum_i (-1)^i V_{ki} c_i^\dagger, \quad (4)$$

where the matrix \mathbf{V} diagonalizes the coupling matrix \mathbf{A} . This enables the expansion of the operator \hat{P} in the eigenbasis as $\hat{P} = \sum_{0 < k \leq L/2} \hat{P}_k$ where $\hat{P}_k = \gamma_k^\dagger \tilde{\gamma}_k + \tilde{\gamma}_k^\dagger \gamma_k$, which exchanges the excitation in each k subspace as $\hat{P}_k \gamma_k^\dagger |0\rangle = \tilde{\gamma}_k^\dagger |0\rangle$. Properties of the operator \hat{P} will be further discussed in the Supplemental Material (SM) [38].

The key point is that for our choice of \hat{P} as the driving term, the chiral disordered model reduces to a collection of two-level systems, e.g., by introducing the ‘‘pseudospin’’ representation $|\uparrow\rangle_k = \gamma_k^\dagger |0\rangle, |\downarrow\rangle_k = \tilde{\gamma}_k^\dagger |0\rangle$, the drive operator \hat{P}_k acts as the σ_x^k operator in each k subspace. According to Eq. (4), the paired excitations have the same spatial wave function up to the $(-1)^i$ phase between neighboring sites. Consequently, the coupling between the paired states via \hat{P}_k will not significantly change the localization properties of the time evolution operator $U(t) = \mathcal{T} \{\exp[-i \int_0^t dt' H(t')]\}$ in the single-particle subspace at any time t for arbitrary forms of the driving profile $f(t)$.

Crucially, this symmetry argument applies only to the single-particle subspace, but not to the multiparticle subspace, in which Eq. (3) generally does not vanish due to the presence of the operator \hat{D} . Although the spectrum for multiple particles remains symmetric, the operator \hat{P} does not simply map between multiparticle paired eigenstates of H_0 , but instead couples many (see SM). Nevertheless, the coupling is highly constrained as the total number of excitations in each k subspace, $N_k = \gamma_k^\dagger \gamma_k + \tilde{\gamma}_k^\dagger \tilde{\gamma}_k$, is a conserved quantity. It trivially commutes with the Hamiltonian H_0 , but it crucially also commutes with \hat{P} which can only convert the excitation at a fixed k but cannot mix different k subspaces [38]. The extensive number of conserved quantities N_k , which are local because of the localized single-particle spectrum of H_0 , can protect many-particle states from delocalization.

This conservation law can be broken by single-particle chiral symmetry-breaking perturbations, e.g., static on-site disorder $\sum_i h_i n_i$ with h_i randomly chosen from $[0, h_{\max}]$. It mixes different k subspaces, hence eigenstates of the time evolution operator $U(t)$ may become delocalized. However, as we will illustrate in the following, if $f(t)$ is periodic or constant, additional potential disorder will not delocalize the system but rather enhance the localization. Delocalization only happens when $f(t)$ is aperiodic, hence highlighting the great importance of the conservation law in protecting the localization especially when TTS is absent.

Numerical results. Although when N_k is conserved, the concrete form of the driving profile $f(t)$ is irrelevant for the persistent localization, here we choose for concreteness the discrete quasiperiodic Thue-Morse (TM) sequence which enables us to probe exponentially long times [20,26,27]. By defining two Hamiltonians

$$H_\pm = H_0 + \sum_i h_i n_i \pm \delta h \hat{P}, \quad (5)$$

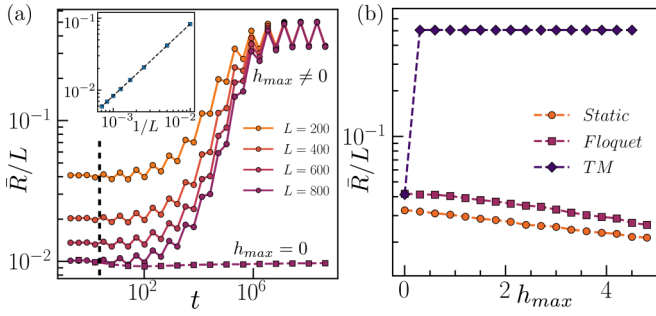


FIG. 1. (a) Average PR for eigenstates of the single-particle time evolution operator U_m at time $t = 2^m T$. Results are calculated for different system sizes and averaged over 100 disorder realization. The PR remains low in the absence of potential disorder, whereas a finite value $h_{\max} = 0.51$ results in delocalization. The inset shows the size dependence of \bar{R}/L at $t \approx 10$ and the scaling $1/L$ is obtained to confirm the localization for short time. (b) PR for the static Hamiltonian, Floquet operator, and TM driving after sufficiently long time $t \approx 10^{12}$ computed for $L = 200$. Potential disorder leads to stronger localization in static and Floquet systems, while any nonvanishing h_{\max} delocalizes the system driven quasiperiodically. We use $J_0 = 1$, $J_{\max} = 1.6\pi$, $\delta h = 1$, $h_{\max} = 0.51$, $1/T = 10$ for the simulation.

one can construct two unitary evolution operators $U_{\pm} = \exp(-iT H_{\pm})$, with the characteristic timescale T . One can recursively define the following unitary operators,

$$U_{n+1} = \tilde{U}_n U_n, \quad \tilde{U}_{n+1} = U_n \tilde{U}_n, \quad (6)$$

with $U_1 = U_- U_+$ and $\tilde{U}_1 = U_+ U_-$. The unitary time evolution for TM drive at stroboscopic times $t_m = 2^m T$ is obtained as $|\psi(t_m)\rangle = U_m |\psi(0)\rangle$ [27]. For Floquet systems, to diagnose the localization properties of single-particle eigenstates, one can use the participation ratio (PR) defined as $R_k = 1/\sum_i |\psi_i^k|^4$, where ψ_i^k denotes the k th eigenfunction at site i of the Floquet operator [39,40]. To quantify the average spreading of the eigenvectors in real space, the average PR is defined over all eigenstates and different disorder realizations $\bar{R} = \langle R_k \rangle_{k,r}$. For general delocalized states, one obtains $\bar{R}/L \sim O(1)$, whereas for perfectly localized ones $\bar{R}/L \sim 1/L$ [40]. However, in contrast to Floquet systems, a time-independent Floquet time evolution operator and its eigenstates are not available for our aperiodic system. Alternatively, $\bar{R}(t)/L$ is computed via the instantaneous eigenstates of the time evolution operator U_m at each stroboscopic time $t = 2^m T$.

As shown in Fig. 1(a), for the case without potential disorder $h_{\max} = 0$, the average PR \bar{R}/L remains at a constant small value indicating that single-particle eigenstates of the evolution operator remain localized. Indeed, for each k subspace, in the long-time limit, the time evolution operator recursively determined by Eq. (6) can be directly diagonalized by $|\uparrow\rangle_k$ and $|\downarrow\rangle_k$, the same eigenstates of the static Hamiltonian H_0 [20,38]. In contrast, the inclusion of potential disorder drastically changes the behavior as different k subspaces start to mix: Following a plateau at low values for finite time $t \sim 10^2$, \bar{R}/L rapidly grows to system size-independent values $[O(1)]$ indicating delocalization. We verified that delocalization occurs for any nonzero value h_{\max} as shown in Fig. 1(b) where the average PR at a long time $t \approx 10^{12}$ is

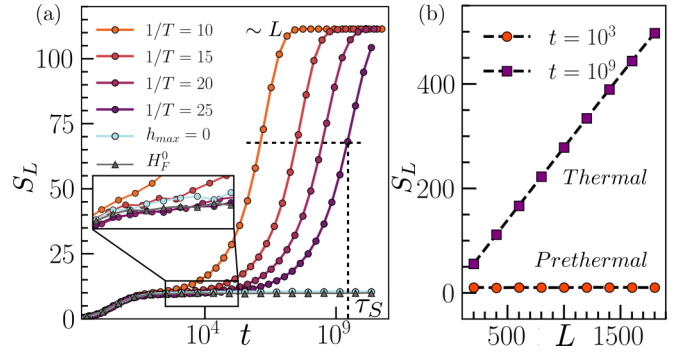


FIG. 2. (a) Entanglement dynamics for different driving rates, with or without potential disorder, averaged over 100 disorder realization and different initial states. Steady state can be delocalized by a nonvanishing potential disorder and thermalized. (b) System size dependence of the entanglement entropy. Prethermal (red dots) and the final plateau (purple squares) exhibit an area- and volume-law scaling, respectively. We use parameters $J_0 = 1$, $J_{\max} = 1.6\pi$, $\delta h = 1$, $h_{\max} = 0.51$, $L = 400$ for the simulation.

plotted. As a comparison, for the Floquet operator $U_- U_+$ and the static Hamiltonian H_+ , the average \bar{R}/L always reduces for larger h_{\max} suggesting that eigenstates are more localized. Such a comparison suggests that the single-particle chiral symmetry protection becomes particularly crucial for aperiodic drives.

To verify the existence of persistent localization in multi-particle systems and to quantify the delocalization crossover at late times in the presence of a potential disorder, we next study the entanglement entropy $S_L(t) = -\text{Tr}[\rho_{L/2} \log_2 \rho_{L/2}]$ with the reduced density matrix $\rho_{L/2}$ of the half chain.

The initial state is chosen as a random product state with zero entanglement in the total magnetization $S_z = 0$ sector (or half filling in the fermionic representation). After switching on the drive, the system starts generating entanglement and its dynamics for varying driving rates $1/T$ is plotted in Fig. 2(a). In the absence of the potential disorder (blue), as eigenstates of U_m always remain localized, entanglement can only be generated within limited regions. Therefore, it saturates around $t \approx 10^2$ at a low value after a transient process, suggesting the appearance of a persistent localized steady state protected by the conservation law of N_k . Once we turn on the potential disorder, localization becomes prethermal with a finite but long lifetime τ_S for large driving rates, e.g., $1/T \geq 15$. This prethermal localization can be well captured by an effective Hamiltonian (gray triangles), $H_{\text{eff}}^0 = (H_+ + H_-)/2$, obtained from the average of the two driving Hamiltonians [26].

As illustrated in the inset, the prethermal plateau (gray triangles) is slightly below the result for the steady state (blue), implying that the additional potential disorder leads to enhanced prethermal localization despite the fact that it eventually delocalizes the system at late times.

The entanglement entropy exhibits a well-pronounced increase after the timescale τ_S towards the final plateau, suggesting the eventual delocalization. As illustrated in Fig. 2(b), in contrast to the prethermal entanglement which is system size independent (orange dots), the final plateau exhibits volume-law scaling (purple squares), demonstrating that entanglement has been established extensively over the whole

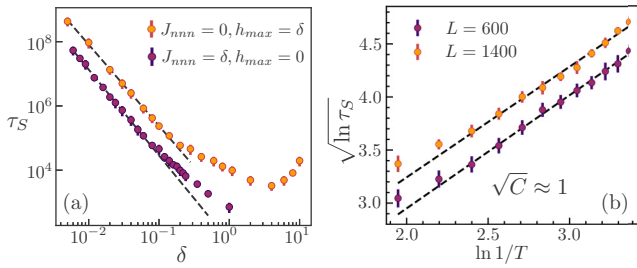


FIG. 3. (a) Algebraic dependence of τ_S on chiral symmetry-breaking perturbation δ with parameter $1/T = 1, L = 1400$. Dashed black lines correspond to the algebraic fit $\delta^{-2.6}$. (b) Delocalization time $\sqrt{\ln \tau_S}$ vs driving rate $\ln 1/T$ with parameter $h_{\text{max}} = 1.1, J_{\text{nnn}} = 0$. The numerical data fit well with a straight line of slope $\sqrt{C} \approx 1$, indicating τ_S behaves as $\tau_S \sim e^{C(\ln(T^{-1}/g))^2}$. Both figures use $J_0 = 1, J_{\text{max}} = 1.6\pi, \delta h = 1$ and 100 disorder average.

system. However, as the system is noninteracting, it does not heat up to infinite temperature. The final entanglement entropy is smaller than the average entropy for a random state, i.e., the Page value $S_\infty = (L \log 2 - 1)/2$ [41].

Prethermal lifetime. For weak breaking of the conservation law delocalization only occurs after a sufficiently long timescale. In Fig. 3(a), we show the dependence of the delocalization time τ_S on different single-particle chiral symmetry-breaking perturbations of strength δ . To quantify the dependence, one can extract the time t_x at which the entanglement entropy crosses the threshold $S_L(t_x)/(L/2) = x$. The prethermal lifetime τ_S is then defined as the average $\tau_S = \langle t_x \rangle_x$ where the averaged is performed by using five different thresholds $x = s_0 \pm \epsilon, s_0 \pm \epsilon/2, s_0$ with the parameter values $s_0 = 0.11$ and $\epsilon = 0.02$.

It is worth noting that the driving frequency ($1/T = 1$) is comparable to other energy scales of H_0 . Hence, the prethermal localization cannot be predicted via a local effective Hamiltonian obtained from a high-frequency perturbative expansion [27]. However, the prethermal localization can still be parametrically long lived as it is protected by approximately conserved quantities N_k . In the case of the small potential disorder $h_{\text{max}} = \delta$ (orange circles), the data fit well with a straight line in the log-log scale, suggesting that τ_S decreases algebraically as $\tau_S \propto \delta^{-\beta}$ with $\beta \approx 2.6$. Interestingly, for $\delta > 0.2$, a clear deviation from the scaling is observed and a turning point appears around $\delta \approx 5$, after which the prethermal lifetime instead increases monotonically. This suggests that beyond this point, instead of playing the role of a symmetry-breaking perturbation, potential disorder stabilizes the localization and prolongs the prethermal lifetime.

Similarly, single-particle chiral symmetry can also be broken by introducing a static next-nearest-neighbor hopping

$J_{\text{nnn}}/2 \sum_i (c_i^\dagger c_{i+2} + c_{i+2}^\dagger c_i)$ to H_0 and approximately the same scaling exponent β is extracted (purple circles). However, in contrast to potential disorder, long-range hopping cannot stabilize the localization, hence no turning point exists.

The prethermal lifetime τ_S also increases with the driving rate $1/T$, and we extract τ_S similar to above, but with $s_0 = 0.13, \epsilon = 0.01$. We plot $\sqrt{\ln \tau_S}$ vs $\ln 1/T$ in Fig. 3(b) for two system sizes with nonzero potential disorder h_{max} . The numerical results fit well with a straight line of slope $\sqrt{C} \approx 1$ in the high-frequency regime, indicating that the prethermal lifetime scales as $\tau_S \sim e^{C(\ln(T^{-1}/g))^2}$ with a local energy scale g as proposed in Ref. [27]. This scaling grows faster than any power law in $1/T$ but slower than exponential [27,38].

Conclusion and discussion. We have identified a persistent localized steady state in a quasiperiodically driven multiparticle noninteracting system. The single-particle chiral symmetry and the resulting conservation law for multiparticle states account for this behavior. One can also add higher powers of the drive operator \hat{P} to the Hamiltonian, which leads to a long-range interaction and precludes the solvability of the model. However, as shown in the SM [38], such an interaction cannot delocalize the system as it preserves the conservation law.

An analogous idea can be readily applied to systems hosting quantum many-body scars [42,43] generated from, for instance, Hilbert space fragmentation [44–47] or a spectrum generating algebra [48–50]. As long as the fragmented structure is preserved by the drive, or the spectrum generating local “ladder” operator [51], which only couples low-entangled scared states, is modulated aperiodically, the system eventually will not thermalize.

The additional potential disorder, which breaks the single-particle chiral symmetry, spoils the conservation law and the system delocalizes after a long prethermal localized regime. Although the dependence of the prethermal lifetime on the driving frequency is well understood for the TM drive, a microscopic description of the delocalization process and its dependence on the symmetry breaking is still missing and worth exploring in the future. In a related vein, a framework for the description of localization in the absence of a natural time-independent time evolution operator—or perhaps a theory of the long-time convergence of the time evolution operators of aperiodic sequences—would be highly desirable.

Acknowledgments. We acknowledge helpful discussion with Simon Lieu and Andrea Pizzi. We acknowledge support from the Imperial-TUM flagship partnership. H.Z. acknowledges support from a Doctoral-Program Fellowship of the German Academic Exchange Service (DAAD). This work was partly supported by the Deutsche Forschungsgemeinschaft under Grant No. SFB 1143 (project-id 247310070) and the cluster of excellence ct.qmat (EXC 2147, project-id 390858490).

[1] A. Lazarides, A. Das, and R. Moessner, Equilibrium states of generic quantum systems subject to periodic driving, *Phys. Rev. E* **90**, 012110 (2014).

[2] D. A. Abanin, W. De Roeck, and F. Huveneers, Exponentially Slow Heating in Periodically Driven

Many-Body Systems, *Phys. Rev. Lett.* **115**, 256803 (2015).

[3] T. Kuwahara, T. Mori, and K. Saito, Floquet–Magnus theory and generic transient dynamics in periodically driven many-body quantum systems, *Ann. Phys.* **367**, 96 (2016).

- [4] A. Lazarides, A. Das, and R. Moessner, Periodic Thermodynamics of Isolated Quantum Systems, *Phys. Rev. Lett.* **112**, 150401 (2014).
- [5] D. A. Abanin and Z. Papić, Recent progress in many-body localization, *Ann. Phys.* **529**, 1700169 (2017).
- [6] A. Lazarides, A. Das, and R. Moessner, Fate of Many-Body Localization Under Periodic Driving, *Phys. Rev. Lett.* **115**, 030402 (2015).
- [7] P. Ponte, Z. Papić, F. Huveneers, and D. A. Abanin, Many-Body Localization in Periodically Driven Systems, *Phys. Rev. Lett.* **114**, 140401 (2015).
- [8] V. Khemani, A. Lazarides, R. Moessner, and S. L. Sondhi, Phase Structure of Driven Quantum Systems, *Phys. Rev. Lett.* **116**, 250401 (2016).
- [9] D. V. Else, B. Bauer, and C. Nayak, Floquet Time Crystals, *Phys. Rev. Lett.* **117**, 090402 (2016).
- [10] P. Titum, E. Berg, M. S. Rudner, G. Refael, and N. H. Lindner, Anomalous Floquet-Anderson Insulator as a Nonadiabatic Quantized Charge Pump, *Phys. Rev. X* **6**, 021013 (2016).
- [11] A. Verdeny, J. Puig, and F. Mintert, Quasi-periodically driven quantum systems, *Z. Naturforsch. A* **71**, 897 (2016).
- [12] P. T. Dumitrescu, R. Vasseur, and A. C. Potter, Logarithmically Slow Relaxation in Quasiperiodically Driven Random Spin Chains, *Phys. Rev. Lett.* **120**, 070602 (2018).
- [13] D. V. Else, W. W. Ho, and P. T. Dumitrescu, Long-Lived Interacting Phases of Matter Protected by Multiple Time-Translation Symmetries in Quasiperiodically Driven Systems, *Phys. Rev. X* **10**, 021032 (2020).
- [14] D. M. Long, P. J. D. Crowley, and A. Chandran, Many-body localization with quasiperiodic driving, *Phys. Rev. B* **105**, 144204 (2022).
- [15] I. Martin, G. Refael, and B. Halperin, Topological Frequency Conversion in Strongly Driven Quantum Systems, *Phys. Rev. X* **7**, 041008 (2017).
- [16] P. J. D. Crowley, I. Martin, and A. Chandran, Topological classification of quasiperiodically driven quantum systems, *Phys. Rev. B* **99**, 064306 (2019).
- [17] S. Körber, L. Privitera, J. C. Budich, and B. Trauzettel, Interacting topological frequency converter, *Phys. Rev. Research* **2**, 022023(R) (2020).
- [18] E. Boyers, P. J. D. Crowley, A. Chandran, and A. O. Sushkov, Exploring 2D Synthetic Quantum Hall Physics with a Quasiperiodically Driven Qubit, *Phys. Rev. Lett.* **125**, 160505 (2020).
- [19] H. Zhao, F. Mintert, and J. Knolle, Floquet time spirals and stable discrete-time quasicrystals in quasiperiodically driven quantum many-body systems, *Phys. Rev. B* **100**, 134302 (2019).
- [20] S. Nandy, A. Sen, and D. Sen, Aperiodically Driven Integrable Systems and Their Emergent Steady States, *Phys. Rev. X* **7**, 031034 (2017).
- [21] B. Lapierre, K. Choo, A. Tiwari, C. Tauber, T. Neupert, and R. Chitra, Fine structure of heating in a quasiperiodically driven critical quantum system, *Phys. Rev. Research* **2**, 033461 (2020).
- [22] X. Wen, R. Fan, A. Vishwanath, and Y. Gu, Periodically, quasiperiodically, and randomly driven conformal field theories, *Phys. Rev. Research* **3**, 023044 (2021).
- [23] D. M. Long, P. J. D. Crowley, and A. Chandran, Nonadiabatic Topological Energy Pumps with Quasiperiodic Driving, *Phys. Rev. Lett.* **126**, 106805 (2021).
- [24] F. Nathan, R. Ge, S. Gazit, M. Rudner, and M. Kolodrubetz, Quasiperiodic Floquet-Thouless Energy Pump, *Phys. Rev. Lett.* **127**, 166804 (2021).
- [25] Z. Qi, G. Refael, and Y. Peng, Universal nonadiabatic energy pumping in a quasiperiodically driven extended system, *Phys. Rev. B* **104**, 224301 (2021).
- [26] H. Zhao, F. Mintert, R. Moessner, and J. Knolle, Random Multipolar Driving: Tunably Slow Heating through Spectral Engineering, *Phys. Rev. Lett.* **126**, 040601 (2021).
- [27] T. Mori, H. Zhao, F. Mintert, J. Knolle, and R. Moessner, Rigorous Bounds on the Heating Rate in Thue-Morse Quasiperiodically and Randomly Driven Quantum Many-Body Systems, *Phys. Rev. Lett.* **127**, 050602 (2021).
- [28] R. Vasseur, A. J. Friedman, S. A. Parameswaran, and A. C. Potter, Particle-hole symmetry, many-body localization, and topological edge modes, *Phys. Rev. B* **93**, 134207 (2016).
- [29] G. De Tomasi, D. Trapin, M. Heyl, and S. Bera, Anomalous diffusion in particle-hole symmetric many-body localized systems, [arXiv:2001.04996](https://arxiv.org/abs/2001.04996).
- [30] D. S. Fisher, Random antiferromagnetic quantum spin chains, *Phys. Rev. B* **50**, 3799 (1994).
- [31] F. J. Dyson, The dynamics of a disordered linear chain, *Phys. Rev.* **92**, 1331 (1953).
- [32] C. M. Soukoulis and E. N. Economou, Off-diagonal disorder in one-dimensional systems, *Phys. Rev. B* **24**, 5698 (1981).
- [33] L. Fleishman and D. C. Licciardello, Fluctuations and localization in one dimension, *J. Phys. C: Solid State Phys.* **10**, L125 (1977).
- [34] G. De Tomasi, S. Roy, and S. Bera, Generalized Dyson model: Nature of the zero mode and its implication in dynamics, *Phys. Rev. B* **94**, 144202 (2016).
- [35] P. Pfeuty, The one-dimensional Ising model with a transverse field, *Ann. Phys.* **57**, 79 (1970).
- [36] J. K. Asbóth, L. Oroszlány, and A. Pályi, The Su-Schrieffer-Heeger (SSH) model, in *A Short Course on Topological Insulators* (Springer, Berlin, 2016), pp. 1–22.
- [37] S. Ryu, A. P. Schnyder, A. Furusaki, and A. W. W. Ludwig, Topological insulators and superconductors: tenfold way and dimensional hierarchy, *New J. Phys.* **12**, 065010 (2010).
- [38] See Supplemental Material at <http://link.aps.org/supplemental/10.1103/PhysRevB.105.L220202> for details regarding the chiral symmetry, localization in the long-time limit, comparison between different fitting methods, and effects of additional interactions.
- [39] S. Roy, I. Khaymovich, A. Das, and R. Moessner, Multifractality without fine-tuning in a Floquet quasiperiodic chain, *SciPost Phys.* **4**, 025 (2018).
- [40] B. Kramer and A. MacKinnon, Localization: theory and experiment, *Rep. Prog. Phys.* **56**, 1469 (1993).
- [41] D. N. Page, Average entropy of a subsystem, *Phys. Rev. Lett.* **71**, 1291 (1993).
- [42] C. J. Turner, A. A. Michailidis, D. A. Abanin, M. Serbyn, and Z. Papić, Weak ergodicity breaking from quantum many-body scars, *Nat. Phys.* **14**, 745 (2018).
- [43] M. Serbyn, D. A. Abanin, and Z. Papić, Quantum many-body scars and weak breaking of ergodicity, *Nat. Phys.* **17**, 675 (2021).
- [44] P. Sala, T. Rakovszky, R. Verresen, M. Knap, and F. Pollmann, Ergodicity Breaking Arising from Hilbert Space Fragmentation

- in Dipole-Conserving Hamiltonians, [Phys. Rev. X **10**, 011047 \(2020\)](#).
- [45] V. Khemani, M. Hermele, and R. Nandkishore, Localization from Hilbert space shattering: From theory to physical realizations, [Phys. Rev. B **101**, 174204 \(2020\)](#).
- [46] A. Hudomal, I. Vasić, N. Regnault, and Z. Papić, Quantum scars of bosons with correlated hopping, [Commun. Phys. **3**, 99 \(2020\)](#).
- [47] H. Zhao, J. Vovrosh, F. Mintert, and J. Knolle, Quantum Many-Body Scars in Optical Lattices, [Phys. Rev. Lett. **124**, 160604 \(2020\)](#).
- [48] S. Moudgalya, N. Regnault, and B. A. Bernevig, Entanglement of exact excited states of Affleck-Kennedy-Lieb-Tasaki models: Exact results, many-body scars, and violation of the strong eigenstate thermalization hypothesis, [Phys. Rev. B **98**, 235156 \(2018\)](#).
- [49] M. Schecter and T. Iadecola, Weak Ergodicity Breaking and Quantum Many-Body Scars in Spin-1 XY Magnets, [Phys. Rev. Lett. **123**, 147201 \(2019\)](#).
- [50] N. Shiraishi and T. Mori, Systematic Construction of Counterexamples to the Eigenstate Thermalization Hypothesis, [Phys. Rev. Lett. **119**, 030601 \(2017\)](#).
- [51] N. O’Dea, F. Burnell, A. Chandran, and V. Khemani, From tunnels to towers: Quantum scars from Lie algebras and q -deformed lie algebras, [Phys. Rev. Research **2**, 043305 \(2020\)](#).